JCTC Journal of Chemical Theory and Computation

Article

pubs.acs.org/JCTC

Solvation Energies of the Proton in Methanol

Jean Jules Fifen,*[,†,‡] Mama Nsangou,[†,§] Zoubeida Dhaouadi,[∥] Ousmanou Motapon,[‡] and Nejm-Eddine Jaidane[∥]

[†]University of Ngaoundere, Faculty of Science, P.O. Box 454, Ngaoundere, Cameroon

[‡]Fundamental Physics Lab, Graduate Training Unit in Physics and Engineering Sciences, Faculty of Science, University of Douala, P.O. Box 24157, Douala, Cameroon

[§]University of Maroua, P.O. Box 46, Maroua, Cameroon

[∥]Laboratoire de Spectroscopie Atomique et Moléculaire, Faculté des Sciences de Tunis, Université de Tunis El Manar, Campus Universitaire 1060, Tunis, Tunisia

Supporting Information

ABSTRACT: pK_a's, proton affinities, and proton dissociation free energies characterize numerous properties of drugs and the antioxidant activity of some chemical compounds. Even with a higher computational level of theory, the uncertainty in the proton solvation free energy limits the accuracy of these parameters. We investigated the thermochemistry of the solvation of the proton in methanol within the cluster-continuum model. The scheme used involves up to nine explicit methanol molecules, using the IEF-PCM and the strategy based on thermodynamic cycles. All computations were performed at B3LYP/6-31++G(dp) and M062X/6-31++G(dp) levels of theory. It comes out from our calculations that the functional M062X is better than B3LYP, on the evaluation of gas phase clustering energies of protonated methanol clusters, per methanol stabilization of neutral methanol clusters and solvation energies of the proton in methanol. The solvation free energy and enthalpy of the proton in methanol were obtained after converging the partial solvation free energy of the proton in methanol and the clustering free energy of protonated methanol clusters, as the cluster size increases. Finally, the recommended values for the solvation free energy and enthalpy of the proton in methanol are −257 and −252 kcal/mol, respectively.

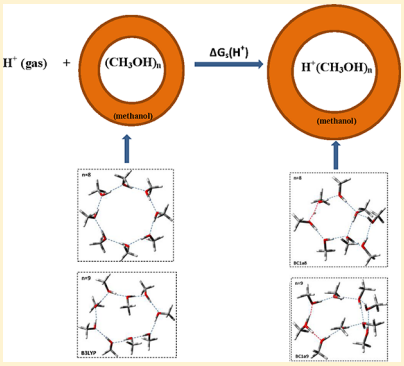

1. INTRODUCTION

Proton-transfer equilibriums are very important for a large variety of chemical compounds and in particular for pharmaceutical products, which frequently are weak acids or bases.[1] Acid dissociation constants (K_a) do not only characterize the acidity of these compounds but also influence their reactivity. They are usually reported as pK_a's, and their values are related to numerous properties of drugs, such as solubility and rate of absorption.[2] They are also taken into account when deciding dosage forms and regimes of drugs.[3] Proton transfer mechanisms are also useful for understanding the antioxidant activity of some chemical compounds. Therefore, accurate knowledge of pK_a's, proton affinities (PAs), and proton dissociation free energies (PDFEs) is highly important for practical purposes as well as for understanding the behavior of chemicals under different conditions.

The calculation of pK_a's, PAs, and PDFEs in proton transfer processes has been subject to extensive studies in computational chemistry.[4−17] The evaluation of these parameters involves quantum chemical calculations of the deprotonation events and the determination of solvation free energies of various species involved. Even with a high computational level of theory, the uncertainty in the solvation free energy of the proton limits the accuracy of these parameters.[4−17] Many authors measured or calculated the solvation free energy of the proton in water.[18−22] They suggested that this value is within −254 to −264 kcal/mol. In contrast to much progress made for evaluating pK_a's, PAs, and PDFEs in aqueous solution, nonaqueous solutions have received far less attention, although they are widely used in chemical reactions.

Early, using the clustering scheme of Tawa et al.,[20] Hwang and Chung[23] calculated the solvation free energy of the proton in methanol. They suggested that this value is −263.4 kcal/mol, stopping the clustering scheme to pentamer methanol structures. This result is arguable and could be revised. Indeed, experimental and recent theoretical results[24−27] suggested that the thermodynamic parameters related to the clustering of neutral or protonated methanol would be saturated for n-mers beyond n = 8. For the purpose of providing highly accurate solvation energies of the proton in methanol, we investigated the structures of protonated and neutral methanol clusters up to n = 9. To this aim, we used two levels of computation and investigated the thermochemical data (clustering energies of protonated methanol clusters and per methanol stabilization energy of neutral methanol clusters) involving the resulting structures.

Received: July 31, 2012
Published: January 10, 2013

Up to now, clusters of protonated water have been of great interest,[28−34] and only very few authors[23−26,35,36] investigated theoretically and experimentally the structure of protonated methanol. Fujii and co-workers[25,26] investigated the infrared (IR) spectroscopy of hydrogen bond networks of protonated methanol clusters, $H^+(CH_3OH)_n$ (n = 4−15) around 160−200 K. They observed the disappearance of the free OH stretching band in the IR dissociation spectra of protonated methanol clusters at n = 7. This would be an indication that, around 160−200 K, the bulk of protonated methanol may be dominated by n-mer structures for which $n \geq 7$. They also observed that the peak position of the broad hydrogen-bonded OH stretch band shows gradual high-frequency shifts with an increase of the cluster size. The blue-shift feature is observed up to n = 9. This is the first reason why we decided to go with clustering up to n = 9, although our investigation stands for the ambient temperature.

Furthermore, the investigation of the structure of liquid methanol has a long history and remains an active research topic.[37,38] Many theoretical studies on this compound have been reported. Monte Carlo and molecular dynamics (MD) simulations were used to study liquid methanol.[39−44] All these methods favor the existence of chains. Wright and El-Shall[44] pointed out that monocyclic, semiplanar structures persist at liquidlike temperatures up to n = 12. *Ab initio* or DFT methods were also used for the same purpose. Previously, Hagemeister et al.[45] carried out B3LYP/6-31+G(d) calculations on methanol clusters $(CH_3OH)_n$ isolated in the gas phase for n = 2−6. Hwang and Chung[23] also investigated the structures of methanol clusters $(CH_3OH)_n$ for n = 1−5 isolated in the gas phase and in methanol, using the B3LYP functional and various basis sets (6-31++G(d,p), cc-PVDZ, cc-PVTZ, aug-cc-PVTZ). Boyd and Boyd[46] also investigated the structures of methanol clusters in the gas phase and at the B3LYP/6-31+G(d) level of computation for n = 2−12. Pires and DeTuri[47] undertook the same computations in the gas phase, investigating PM3, HF, B3LYP, MP2, and ONIOM methods and 6-31G(d), 6-31+G(d,p), and 6-311++G(d,p) basis sets. All *ab initio* or DFT methods lead to the same result as molecular mechanics (MM) methods: the cyclic methanol clusters are the global minima structures as compared to chain, branched-cyclic, and branched-chain arrangements. Ohno et al.[48] also found experimentally that the cyclic conformer is the most stable structure of all conformers investigated. Moreover, Krishtal et al.[27] calculated the polarizability of methanol clusters at the B3LYP/6-311++G(d,p) level of computation. The authors found that the molecular polarizability decreases with the size of the cluster and stabilizes at a value around 15.3 au only at larger clusters of aggregation, 9−10. This suggests the investigation of n-mers of neutral methanol clusters, at least, up to n = 9. Therefore, in the present work, we investigated only the cyclic methanol clusters $(CH_3OH)_n$, n = 1−9, isolated in the gas phase and methanol. It is worth mentioning that, up to now, before our present work, the only available structures of protonated or neutral methanol clusters in methanol were those pointed out by Hwang and Chung,[23] for n = 1−5.

2. COMPUTATIONAL DETAILS

2.1. Solvation Energies of the Proton. One way to calculate the solvation free energy of the proton in methanol ($\Delta G_s(H^+)$), is to converge the free energy change of the following reaction

$$H^+(gas) + (CH_3OH)_n(gas) \rightarrow H^+(CH_3OH)_n(gas) \quad (1)$$

by increasing n, the size of the cluster. The index s denotes the solvent and stands here for methanol. The calculation of $\Delta G_s(H^+)$ by following the above-described scheme is extremely difficult in several respects. First, it involves the determination of the structures of neutral, $(CH_3OH)_n$, and protonated, $H^+(CH_3OH)_n$, methanol clusters for large values of n. In regard to the case of water clusters,[49] even with the structures in hand, the free energy is slowly convergent as the size of the cluster increases. The calculations of these latter parameters at a high *ab initio* or DFT level would be computationally intense and would become prohibitively long with large basis sets.

To overcome this difficulty, we used in this work a similar scheme to that proposed by Tawa et al.,[20] representing the proton hydration. Thus, the proton solvated in methanol is represented by the following model process (see eq 2 and Figure 1):

$$H^+(gas) + (CH_3OH)_n(methanol) \rightarrow H^+(CH_3OH)_n(methanol) \quad (2)$$

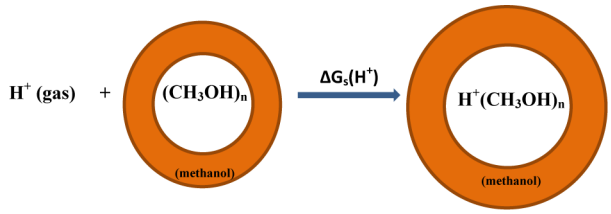

Figure 1. Schematic description of the solvation of the proton in methanol.[20] The reactants are the neutral n-mer methanol cluster embedded in a dielectric continuum methanol solvent and a bare proton. The product is a protonated n-mer methanol cluster embedded in the same medium. The colored areas represent the bulk of methanol molecules described as a dielectric continuum medium.

and again converges the free energy change of the above equation, by increasing n. This free energy change is interpreted as the partial solvation free energy of the proton, and noted $\Delta G_s(H^+)_n$. Thus, the solvation free energy of the proton is calculated as

$$\Delta G_s(H^+) = \lim_{n\rightarrow\infty} \Delta G_s(H^+)_n \quad (3)$$

(methanol) is intended to represent the particular species embedded in a bulk of methanol molecules described as a dielectric continuum medium. The same procedure is applied for the solvation enthalpy of the proton in methanol, $\Delta H_s(H^+)$.

The assumption is that explicit methanol molecules are not necessary for representing the bulk solvent; a dielectric continuum model should be sufficient. That being the case, then n should not have to be too large to converge the free energy change associated with eq 1. In this model, the solvent at $n\rightarrow\infty$ is replaced by neutral methanol cluster, $(CH_3OH)_n$, embedded in a dielectric continuum where n now is a small number in the range of 5−9. The solvated proton at $n\rightarrow\infty$ is replaced by the $H^+(CH_3OH)_n$ supermolecule complex embedded in a dielectric continuum medium where n is the same as for the modeled solvent. Thus, $\Delta G_s(H^+)_n$ and $\Delta H_s(H^+)_n$ are calculated respectively with the eqs 4 and 5.

$$\Delta G_s(H^+)_n = \Delta G_s[H^+(CH_3OH)_n] - \Delta G_s[(CH_3OH)_n] - \Delta G_{gas}(H^+) \quad (4)$$

$$\Delta H_s(H^+)_n = \Delta H_s[H^+(CH_3OH)_n] - \Delta H_s[(CH_3OH)_n] - \Delta H_{gas}(H^+) \quad (5)$$

Since the free energy of a species X in a solvent ($\Delta G_s(X)$) can be defined as the sum of its free energy in the vacuum ($\Delta G_{gas}(X)$) and its free solvation energy ($\Delta\Delta G_s(X)$), eq 4 can be rewritten as

$$\Delta G_s(H^+)_n = \Delta G_{gas}[H^+(CH_3OH)_n] - \Delta G_{gas}[(CH_3OH)_n] - \Delta G_{gas}(H^+) + \{\Delta\Delta G_s[H^+(CH_3OH)_n] - \Delta\Delta G_s[(CH_3OH)_n]\} \quad (6)$$

The last two terms of this equation are simply noted $\Delta(\Delta\Delta G_s)_n$ and stands for the difference in solvation free energies of protonated methanol and neutral methanol clusters. Thus,

$$\Delta(\Delta\Delta G_s)_n = \Delta\Delta G_s[H^+(CH_3OH)_n] - \Delta\Delta G_s[(CH_3OH)_n] \quad (7)$$

By definition, $\Delta(\Delta\Delta G_s)_n$ is an increasing negative and zero-convergent suite. When $\Delta(\Delta\Delta G_s)_n = 0$, eq 1 can be replaced by eq 2, and one can use a limited number of explicit methanol molecules in order to converge the solvation free energy of the proton without using bulk solvent to do it.

It is worth noting that before converging the partial solvation free energy of the proton in methanol, one should first ensure the convergence of the clustering free energy of the protonated methanol in the gas phase. Clustering energies of the protonated methanol can be evaluated using the following equation:

$$CH_3OH + H^+(CH_3OH)_{n-1} \rightarrow H^+(CH_3OH)_n \quad (8)$$

For simplification, we used the notation MeOH and H^+MeOH for neutral methanol and protonated methanol, respectively. Prior to the detailed descriptions of the free energy-optimized conformer structures of $H^+(MeOH)_n$, a brief summary of the possible coordination types of MeOH and H^+MeOH sites and morphological types of $H^+(MeOH)_n$ as introduced by Fujii and co-workers[25,26] are presented in the following subsection.

2.2. Coordination Types of MeOH and H^+MeOH. Figure 2 shows the symbolic representations of the possible coordination types for the MeOH and H^+MeOH sites according to their coordination numbers. On one-coordinated sites, a MeOH can either be an A (proton acceptor) or a D (proton donor) site. On two-coordinated sites, a MeOH can take the form of an AA (double-acceptor) or an AD (single acceptor single donor). A three-coordinated site of a MeOH is uniquely an AAD (double acceptor single donor). Different from the case of water, an ADD (single acceptor double donor) site is prohibited for MeOH because of the lack of the second proton to donate.

For a H^+MeOH, a one-coordinated A or D site and a two-coordinated AD or AA site are energetically not favorable (except for very small clusters) as the hydrogen bond between the ion core and neighboring MeOH molecules is stronger than the hydrogen bonds between two neutral MeOH molecules. As a result, the ion core would like to donate both of its protons.

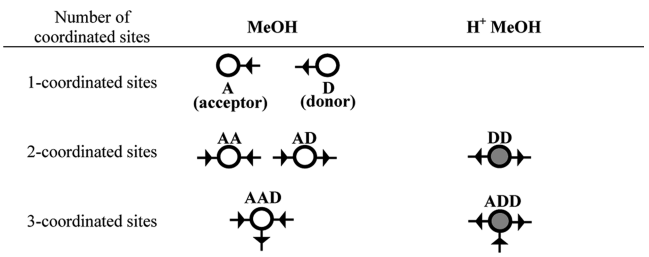

Figure 2. Symbolic representations of the possible coordination types of the MeOH and H^+MeOH sites.[25] All the methyl groups and hydrogen atoms were omitted in this representation. The oxygen atom is represented by an open circle and a gray circle on MeOH and H^+MeOH, respectively. An arrow indicates the hydrogen bond that binds two oxygen atoms. The direction of the arrow shows the donor−acceptor relation in the hydrogen bond.

This tendency was verified early by Chang and co-workers.[35,36] Thus, the coordination type is either a two-coordinated DD (double donor) site or a three-coordinated ADD (single acceptor double donor) site. However, Fujii et al.[25] found that the latter form is not stable. They also showed that according to coordination types of H^+MeOH sites, only five basic types of H^+MeOH can be constructed:[25,26] linear (L), cyclic (C), cyclic with a tail (Ct), first type of bicyclic (BC1), and second type of bicyclic (BC2), Figure 3. From a structural (not topological)

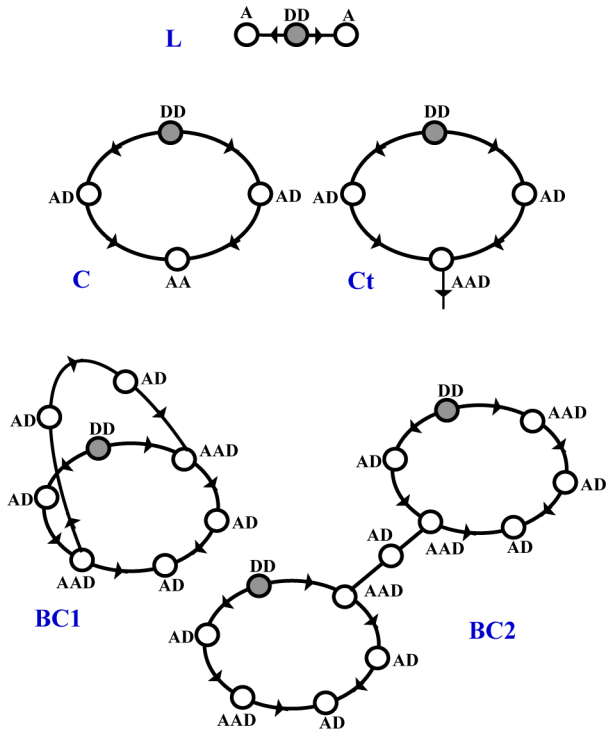

Figure 3. Schematic representations of the five basic morphologies of $H^+(MeOH)_n$.[25] The same conventions as those used in Figure 2 were adopted here. One may add and remove one or more AD molecules.

viewpoint, Fujii and co-workers[25,26] suggested that BC1 can further be divided into two groups: BC1a and BC1b. In BC1a, the shortest hydrogen bond network directly connects both three-coordinate (AAD) molecules without any AD molecules included. In BC1b, all the three hydrogen bond lines have at least one AD molecule.

dx.doi.org/10.1021/ct300669v | J. Chem. Theory Comput. 2013, 9, 1173−1181

2.3. Computational Level of Theory. The dielectric continuum medium was modeled using the integral equation formalism polarized continuum model (IEF-PCM).[50] All thermochemistry data were computed at a temperature of 298.15 K and a pressure of 1 atm. Geometry optimizations were carried out using the density functional theory (DFT) methods implemented in the Gaussian 09 computational package.[51]

DFT was chosen because of the excellent compromise between the computational time and the description of the electronic correlation. In all calculations performed in this work, B3LYP and M062X functionals were used. The B3LYP functional is the famous functional which consists of Becke's three parameters exact exchange functional (B3)[52] combined with the nonlocal gradient corrected correlation functional of Lee−Yang−Parr (LYP).[53] The M062X[54] functional is a highly nonlocal functional with double the amount of nonlocal exchange (2X). This functional is designed to be suitable for a combination of main group thermochemistry, kinetics, and noncovalent interactions.[54] This functional is one of the few functionals that has been developed especially to handle van der Waals interactions and has demonstrated excellent results for these types of systems.[15,55,56] The basis set used in this work was 6-31++G(d,p).[57−59] Full tight geometry optimization was carried out without symmetry constraints up to the convergence. All numerical integrals were computed with the ultrafine grid, in order to overcome low frequency modes induced by methyl rotations. A subsequent vibrational frequency calculation was undertaken in order to confirm that the resulting equilibrium geometries were minima (no negative frequency) on the potential energy surface (PES).

Within this work, data fitting was performed using the Levenberg−Marquardt method.[60,61]

3. RESULTS AND DISCUSSION

3.1. Clustering of Protonated Methanol Clusters. Concerning the protonated methanol clusters, we investigated in our previous work[62] all the possible morphologies for each cluster size in the vacuum and in solvent. The computational methods used were M062X and B3LYP/6-31++G(d,p). Therein, for each cluster size, the relative stability of all possible structures obtained as well as temperature effects were clearly discussed. Similar structures were found with both computational methods. From this work, we found that at 298.15 K, in the gas phase and at both levels of computation (B3LYP and M062X), the linear structures were favored up to n = 8, and for n = 9, the more stable morphology was Ct9. The behavior is very different in methanol as a solvent. In fact, the structures favored in methanol at the M062X level of computation were L3, L4, C5, Ct6, C7, C8, and C9 for n = 3−9, respectively. Those favored at the B3LYP level of computation were linear structures for each cluster size, except for n = 6 where the structure favored was Ct6. All the favored structures in both media and at both levels of computation are depicted in Figure 4. The Cartesian coordinates of all these structures were provided in annex1 (see Supporting Information).

Clustering energies, clustering enthalpies, and clustering free energies of protonated methanol clusters for n = 2−9 were computed using eq 8 in the gas phase, at the B3LYP/6-31++G(d,p) and M062X/6-31++G(d,p) levels of computation. The results obtained were summarized in Table 1. Previously, Chang et al.[35] calculated the clustering energies of protonated

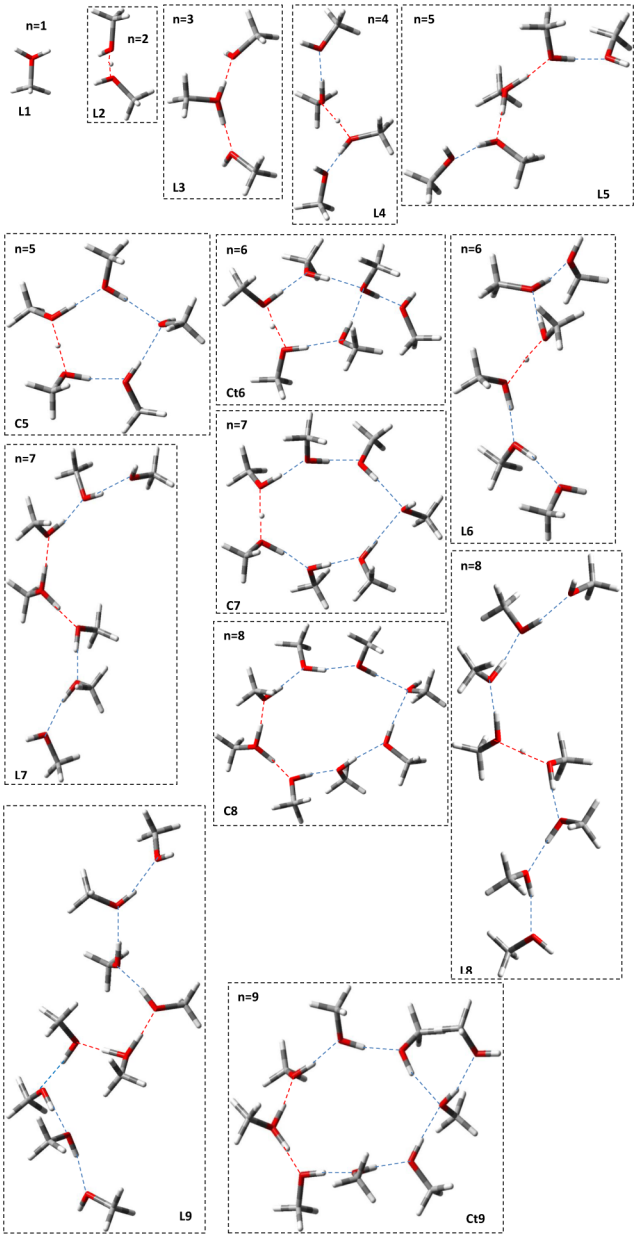

Figure 4. The more stable structures of protonated methanol clusters $(H^+(MeOH)_n$, n = 1−8).

methanol clusters at the B3LYP/6-31+G(d) level of computation, for n = 2−5. Our calculations using B3LYP and M062X are consistent with those published by these authors for n = 2−5, Figure 5.

In addition, our two computational levels lead to the result that the clustering energy of protonated methanol increases with the cluster size and saturates at n = 8 or 9. This may be an indication that at 0 K, the clustering of $H^+(MeOH)_n$ should be stopped at n = 8 or 9.

The calculated clustering enthalpies are very similar to those related to clustering energies, Figure 6. Results are very consistent with those of Chang et al.[35] for n = 2−5. Although our results obtained with both levels of computation are closer to the experimental results of Grimsrud and Kebarle,[24] M062X results are better than those from B3LYP. This could be explained by the fact that the B3LYP functional fails to describe dispersion interactions and deprotonation processes, which are

Table 1. Calculated Clustering Energies ($\Delta E_{n-1,n}$), Clustering Enthalpies ($\Delta H_{n-1,n}$) and Clustering Free Energies ($\Delta G_{n-1,n}$) of Protonated Methanol Molecules $H^+(MeOH)_n$, at B3LYP/6-31++G(d,p) and M062X/6-31++G(d,p) Levels of Computation and Experimental Data at 300 K[a]

	B3LYP/6-31++G(d,p)			M062X/6-31++G(d,p)			experiment[24]		
$n-1,n$	$\Delta E_{n-1,n}$	$\Delta H_{n-1,n}$	$\Delta G_{n-1,n}$	$\Delta E_{n-1,n}$	$\Delta H_{n-1,n}$	$\Delta G_{n-1,n}$	$\Delta H^\circ_{n-1,n}$	$\Delta H^\circ_{n-1,n}$	$\Delta G^{\circ,Fit}_{n-1,n}$
1,2	−34.8	−35.0	−25.7	−36.7	−37.0	−27.9	−33.1	−24.0	−24.0
2,3	−21.0	−18.6	−11.3	−22.2	−20.0	−11.6	−21.3	−12.9	−12.7
3,4	−15.4	−14.9	−5.7	−17.0	−16.5	−9.1	−16.1	−7.5	−7.7
4,5	−12.9	−10.4	−2.9	−14.4	−12.0	−4.1	−13.5	−4.9	−4.9
5,6	−12.0	−10.1	−2.6	−13.9	−11.9	−3.9	−12.5	−3.2	−3.2
6,7	−9.6	−8.0	−0.7	−12.0	−9.8	−2.1	−11.9	−2.1	−2.1
7,8	−10.8	−8.0	0.9	−12.9	−10.2	−2.0	−12.0	−1.4	−1.3
8,9	−10.4	−8.9	5.5	−13.2	−11.5	2.9			−0.8

[a]All energies are in kcal/mol. $\Delta G^{\circ,Fit}_{n-1,n}$ is the fitted data of $\Delta G^\circ_{n-1,n}$.

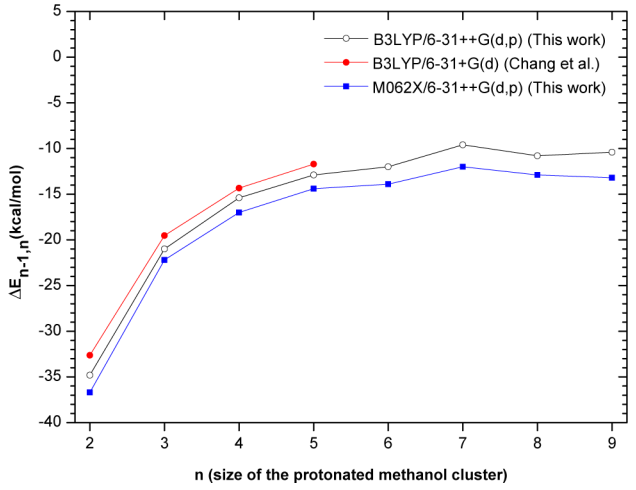

Figure 5. Gas phase clustering energies of protonated methanol clusters, $H^+(MeOH)_n$ for $n = 2-9$.

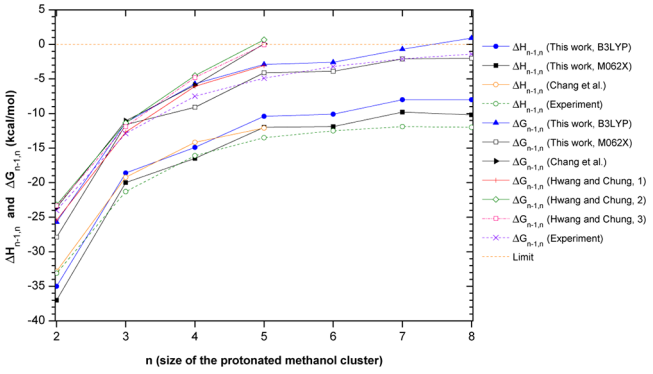

Figure 6. Gas phase clustering enthalpies and free energies of protonated methanol clusters, $H^+(MeOH)_n$ for $n = 2-9$. Since the experimental value of $\Delta G_{8,9}$ was not available, it was estimated by a fit procedure from the experimental values of $\Delta G_{n-1,n}$, $n \leq 8$. In the legend, the numbers 1, 2, and 3 after Hwang and Chung names denote the computational levels B3LYP/6-31++G(d,p), B3LYP/aug-cc-PVDZ, and B3LYP/aug-cc-PVTZ, respectively, used by these authors. The experiment results were published by Grimsrud and Kebarle.[24]

somewhat encompassed by the other functional. The failure of B3LYP on the description of deprotonation processes could be found in the works of Shields and colleagues.[63−67] Our results obtained with both computational levels show that the clustering enthalpy of $H^+(MeOH)_n$ increases with n and saturates at $n = 7$.

Chang et al.[35] and Hwang and Chung[23] calculated the clustering free energies of $H^+(MeOH)_n$ for $n = 2-5$. Hwang and Chung used 6-31++G(d,p), cc-PVDZ, aug-cc-PVDZ, cc-PVTZ, and aug-cc-PVTZ basis sets without including zero-point energy (ZPE) corrections in their calculations, except for aug-cc-PVTZ basis sets. For the purpose of avoiding redundance, only their results related to the first three basis sets were retained and depicted in Figure 6. Our B3LYP results on clustering free energies are consistent with those pointed out by both groups of authors. The agreement with experimental results[24] is excellent, considering the 10% accuracy of the experimental results. However, according to the results of Hwang and Chung, B3LYP/6-31++G(d,p) calculated values without ZPE corrections would give better agreement than those obtained by using other basis sets. This is why we chose the basis set 6-31++G(d,p) in this work.

The experimental clustering free energies behave quite regularly as the cluster size increases and can be fitted by eq 9

$$\Delta G^{exptl.}_{n-1,n} = (a_1 + a_2 \ln(n))n^{a_3} \quad (9)$$

where the parameters were set as $a_1 = -63.120$, $a_2 = 26.146$, and $a_3 = -0.904$ in kcal/mol. The fitted curve is depicted in Figure 7. The fitted data reproduce excellently the experimental

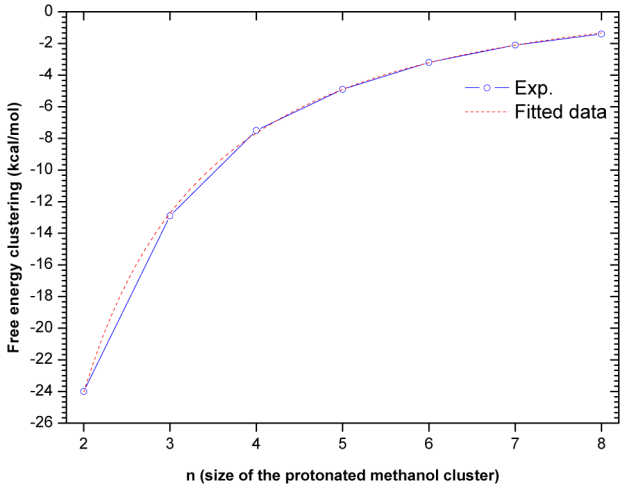

Figure 7. Fitted curve of the experimental free energies of protonated methanol clusters.

dx.doi.org/10.1021/ct300669v | J. Chem. Theory Comput. 2013, 9, 1173−1181

ones. From the analytic expression of $\Delta G^{exptl.}_{n-1,n}$, the value at $n = 9$ was estimated to be −0.8 kcal/mol, Table 1. This value also reported in Figure 6 is very close to the value obtained at $n = 8$ with the difference of 0.5 kcal, which is within the computational error. Thereby, the convergence of $\Delta G^{exptl.}_{n-1,n}$ at $n = 9$ would lead to reliable physical insights. Furthermore, the estimated values of $\Delta G^{exptl.}_{n-1,n}$ for $n = 10$, 11, and 12 were −0.4, −0.05, and 0.2 kcal/mol, respectively. Thus, the strict convergence of this parameter would be reached at $n = 11$. Unfortunately, clustering up to this value is not practically possible for at least two reasons. First, going so far in DFT computational level would consume prohibitive time. Even though the structures are obtained at this computational level, they may lead to nonreliable results, since beyond $n = 9$, $\Delta G^{exptl.}_{n-1,n}$ may be under the computational error range and sensitive to entropic errors due to rotations of methyl groups. Therefore, at the DFT computational level, the number of explicit methanol molecules to converge the clustering free energy of protonated methanol and, thereafter, the partial solvation free energy of the proton is $n = 9$. This is also a strong justification of our decision to stop clustering of protonated methanol at $n = 9$ for the accurate evaluation of solvation energies of the proton in methanol. It is worth mentioning that the M062X functional leads to better agreement with experimental results as compared to B3LYP. The high positive clustering free energies noted at $n = 9$ with both levels of computation could be ascribed to entropic errors due to rotations of methyl groups. Thus, the partial solvation enthalpies and free energies for $n = 9$ were obtained by an extrapolation. In fact, these values were derived in regard to fitted curves obtained for $n = 1$−8.

3.2. Clustering of Neutral Methanol and Determination of $\Delta(\Delta G_s)_n$. Geometry optimizations of isolated methanol clusters $(MeOH)_n$, $n = 1 - 9$ were carried out at both levels of computation, in gas phase and methanol. Based on previous works[23,39−48,68] which present cyclic methanol clusters as the more stable conformers among all possible structures (linear, cyclic with tail, bicyclic, ...) of methanol clusters, only the cyclic structures were investigated for $n = 3 - 9$. The more stable structures obtained were based on the minimum zero-point corrected free energy. Very similar structures were obtained in both levels of computation in gas phase as in methanol, except for nonamer structure obtained with M062X functional. Thus, only structures obtained in the gas phase at M062X/6-31++G(d,p) were depicted in Figure 8, except for $n = 9$ with M062X where structures obtained in both media were also depicted. The coordinates of these structures were provided in annex2 (see the Supporting Information). All these structures are consistent with those pointed out by other authors.[23,45−48,68,69]

Per methanol stabilization energy (ΔE_n) of the neutral methanol cluster of size n was computed using B3LYP and M062X levels of computation using the formula

$$\Delta E_n = \frac{E_n}{n} - E_1 \qquad (10)$$

where E_n is the zero-point corrected electronic energy of the n-mer, and E_1 is the zero-point corrected electronic energy of the monomer. From the calculated values (ΔE_n), one may derive that the methanol clusters become stable for $n = 6$ (see Figure 9 or Table S1 in the Supporting Information). M062X values are better than B3LYP ones, since the former results are the closest to the value of the vaporization enthalpy of methanol (−9.2 kcal/mol[70]). Elsewhere, we stopped the clustering of neutral methanol at $n = 9$, since the stabilization of the molecular polarizability of neutral methanol clusters is reached at that value of the cluster size.[27]

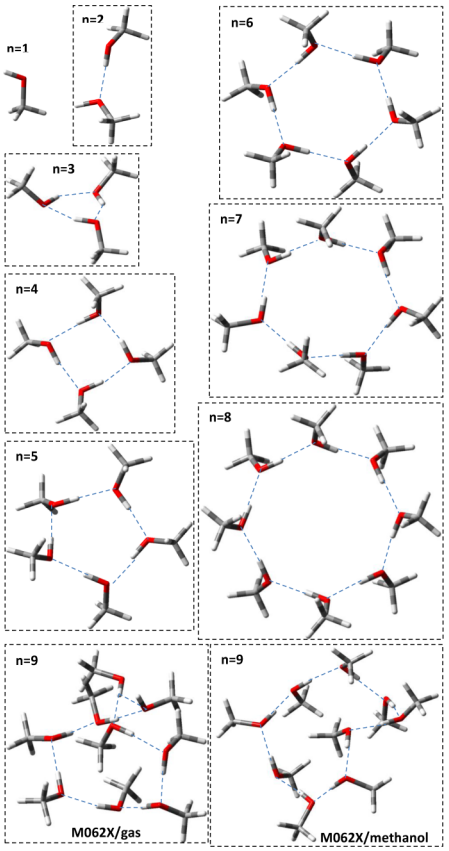

Figure 8. The more stable structures of neutral methanol clusters ($(MeOH)_n$, $n = 1$−9) obtained at the M062X/6-31++G(d,p) computational level. Very similar structures were also obtained at the B3LYP/6-31++G(d,p) computational level. For $n = 1$−8, the structures obtained in the gas phase and in methanol are very similar. The dashed lines represent hydrogen bonds.

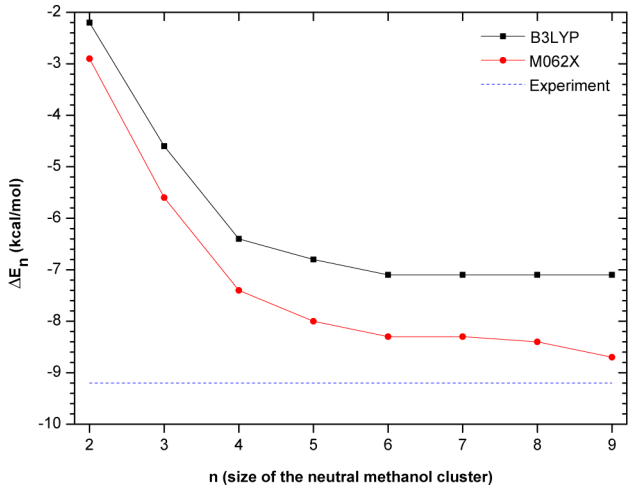

Figure 9. Per methanol stabilization energy of gas phase neutral methanol clusters, at B3LYP and M062X/6-31++G(d,p).

The differences in solvation free energies of protonated methanol and neutral methanol clusters ($\Delta(\Delta G_s)_n$) were evaluated for various cluster sizes. Due to the good similarity of

results in our computations, only M062X results were depicted in Figure 10. For the purpose of predicting the number of

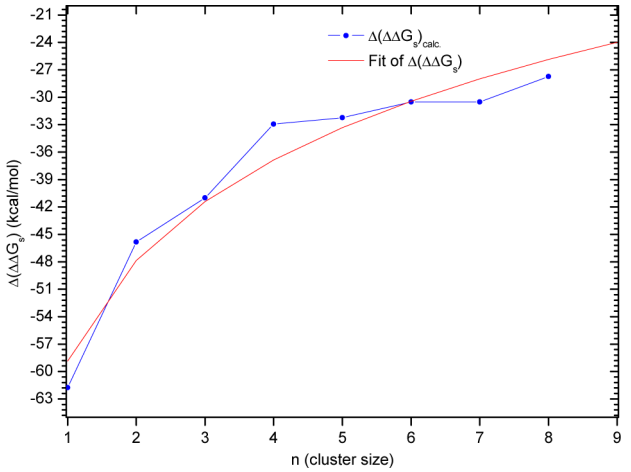

Figure 10. Difference in solvation free energies of protonated methanol and neutral methanol clusters. The red line is the fitted curve from calculated values to a logarithmic function.

explicit methanol molecules to be used to converge the solvation free energy of the proton without using bulk solvent (replacing eq 2 by eq 1), $\Delta(\Delta\Delta G_s)_n$ data were fitted to a logarithmic function (Figure 10) defined by eq 11

$$\Delta(\Delta\Delta G_s)_n = b_1 + b_2 \ln(n) \quad (11)$$

where $b_1 = -58.851$ kcal/mol and $b_2 = 15.862$ kcal/mol. The fitted curve reproduces very well the trend of the curve of $\Delta(\Delta\Delta G_s)_n$. Moreover, solving the equation $\Delta(\Delta\Delta G_s)_n = 0$ leads to $n = 41$, which is unrealistic at the DFT or *ab initio* level of theory. This is a confirmation that the scheme of Tawa used to derive solvation energies of the proton in methanol is still being practical and realistic at the DFT or *ab initio* computational level.

3.3. Solvation Energies of the Proton in Methanol. With protonated and neutral methanol clusters in hand, we were able to evaluate solvation free energy and enthalpy of the proton in methanol. The calculated partial solvation free energies and enthalpies of the proton in methanol were summarized in Table S2 (in the Supporting Information) and depicted in Figure 11. These thermodynamic parameters decrease with the cluster size and saturate from $n = 7$. This trend is consistent with clustering thermodynamic parameters evaluated early in this work. The exception is noted for $\Delta G_s^{M062X}(H^+)_n$, for which the saturation is not clearly presented.

Furthermore, the solvation enthalpies and free energies of the proton in methanol behave quite regularly as the cluster size increases and may be fitted using the exponential function (Figure 11) as defined below:

$$\Delta H_s^{B3LYP}(H^+)_n = c_1 + c_2 \exp(c_3 n) \quad (12)$$

$$\Delta H_s^{M062X}(H^+)_n = c_1' + c_2' \exp(c_3' n) \quad (13)$$

$$\Delta G_s^{B3LYP}(H^+)_n = d_1 + d_2 \exp(d_3 n) \quad (14)$$

$$\Delta G_s^{M062X}(H^+)_n = d_1' + d_2' \exp(d_3' n) \quad (15)$$

where $c_1 = -257.986$, $c_2 = 90.848$, $c_3 = -1.334$, $c_1' = -250.913$, $c_2' = 93.794$, $c_3' = -1.331$, $d_1 = -250.697$, $d_2 = 82.961$, $d_3 = -1.242$, $d_1' = -255.103$, $d_2' = 54.864$, and $d_3' = -0.675$ in kcal/mol. The fitted data reproduce very well the calculated data and remain constant for $n \geq 8$, especially for B3LYP results. Fitted data confirm that any clustering of neutral or protonated methanol beyond $n = 9$ may not be necessary. Therefore

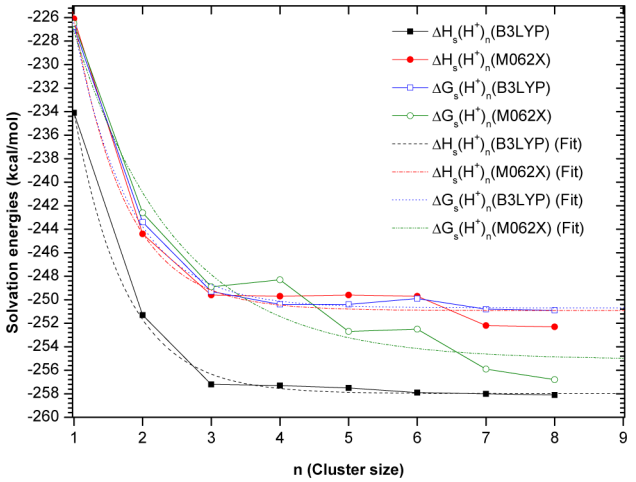

Figure 11. Partial solvation energies of the proton versus the cluster size, in methanol. The dashed lines are the fits of the calculated values.

$$\Delta H_s^{B3LYP}(H^+) = \Delta H_s^{B3LYP}(H^+)_8 = -259 \text{ kcal/mol} \quad (16)$$

$$\Delta H_s^{M062X}(H^+) = \Delta H_s^{M062X}(H^+)_8 = -252 \text{ kcal/mol} \quad (17)$$

$$\Delta G_s^{B3LYP}(H^+) = \Delta G_s^{B3LYP}(H^+)_8 = -251 \text{ kcal/mol} \quad (18)$$

$$\Delta G_s^{M062X}(H^+) = \Delta G_s^{M062X}(H^+)_8 = -257 \text{ kcal/mol} \quad (19)$$

On the basis of the convergence at $n = 8$ or 9 for all thermodynamic clustering parameters (clustering energy, clustering enthalpy, and clustering free energy) involved in this work, solvation free energy and enthalpy of the proton in methanol may be better estimated using *octamer* or *nonamer* clusters of neutral and protonated methanol. In regard to the best agreement of M062X results with experimental ones in all thermodynamic clustering parameters involved in this work, we strongly recommend results from M062X computations. Furthermore, it is noteworthy that the solvation free energies obtained with both levels of computation are comparable to the value obtained (−263.5 kcal/mol) by Kelly et al.,[71] using the cluster pair approximation method. They are also comparable to the hydration free energy which is suggested to be within −259 to −264 kcal/mol.[4,18−22] From B3LYP results, the solvation free energy of the proton in methanol was improved by about 0.5 kcal/mol, shifting the limit clustering from $n = 5$ to $n = 9$. Thus, was it necessary to go farther in DFT computational level? The answer may be positive. In fact, such an extension induces an error of 0.4 pK_a unit, which is acceptable. Thereafter, such an error would be insignificant in regard to the proton affinity or proton dissociation free energy. Although this error would not affect hydrogen bonds, it would seriously affect van der Waals interactions and lead to erroneous binding energies. Elsewhere, one could have stopped the clustering early by considering only the convergence of the solvation free energy as proposed by Tawa[20] in the case of water as a solvent. In this way, with our M062X results, the convergence would have been reached at $n = 4$, and the solvation free energy of the proton in methanol would have

been −249.7 kcal/mol, Table S2. The error on such a result would have been 7.1 kcal. Such an error would badly describe hydrogen bonds and would lead to an unacceptable error of 5.2 pK_a units. Using our B3LYP results, the convergence would have been serendipitous at $n = 4$ or $n = 5$. Therefore, ensuring only the convergence of the partial solvation free energy, to evaluate the solvation free energy of the proton in methanol would depend on the computational method. A reliable way to overcome this difficulty is to converge the free energy clustering of protonated methanol clusters before converging the partial solvation free energy of the proton in methanol.

4. CONCLUSION

In this work, we investigated the thermochemistry of the solvation of the proton in methanol within the cluster-continuum model. The scheme used involves up to nine explicit methanol molecules, using the IEF-PCM and the strategy based on thermodynamic cycles. Two DFT functionals (B3LYP and M062X) have been investigated with the 6-31++G(d,p) basis sets.

By converging all the gas phase thermodynamic clustering parameters, we found that nine explicit methanol molecules are sufficient to derive accurate solvation free energy or enthalpy of the proton in methanol. Thus, it may not be recommended to go beyond this cluster size, neither to investigate the clustering thermochemistry of neutral or protonated methanol nor to investigate the solvation free energy or enthalpy of the proton in methanol.

It is useful to note that, ensuring only the convergence of the partial solvation free energy, to evaluate the solvation free energy of the proton in methanol would depend on the computational level and would not be sufficient. A reliable way to overcome this difficulty is to converge the free energy clustering of protonated methanol clusters before converging the partial solvation free energy of the proton in methanol.

We have also shown that the M06-2X functional gives better results than the B3LYP functional for gas phase clustering energies of protonated methanol clusters, for per methanol stabilization energy of neutral methanol clusters, and for the estimation of the solvation energies of the proton in methanol. The recommended values of the solvation free energy and enthalpy of the proton in methanol are −257 and −252 kcal/mol, respectively.

■ ASSOCIATED CONTENT

Supporting Information

Per methanol stabilization energies for neutral methanol clusters, partial solvation free energies and enthalpies of the proton in methanol, and optimized Cartesian coordinates of all conformers of neutral and protonated methanol structures. This material is available free of charge via the Internet at http://pubs.acs.org.

■ AUTHOR INFORMATION

Corresponding Author

*Tel.: 00237 7521 6139. E-mail: julesfifen@gmail.com.

Notes

The authors declare no competing financial interest.

■ ACKNOWLEDGMENTS

The authors thank the Abdus Salam ICTP for their financial support to this work through the OEA-NET 45 project. J.J.F. particularly thanks Prof. Kwato Njock Moïse Godffroy for facilitating his enrolment in the aforementioned project. He also thanks Prof. Emeritus Zohra Ben Lakhdar (University of Tunis El Manar, Tunisia) and Prof. Souad Chekir Lahmar (University of Carthage, Tunisia) for their warm hospitality in Tunisia where this work was achieved.

■ REFERENCES

(1) Riccardi, D.; Schaeffer, P.; Cui, Q. *J. Phys. Chem. B* **2005**, *109*, 17715−17733.
(2) Brown, T. N.; Mora-Diez, N. *J. Phys. Chem. B* **2006**, *110*, 9270−9279.
(3) Thomas, G. *Medicinal Chemistry: An Introduction*; John Wiley Sons: West Sussex, U.K., 2000.
(4) Ho, J.; Coote, M. L. *J. Chem. Theory Comput.* **2009**, *5*, 295−306.
(5) Liptak, M. D.; Shields, G. C. *J. Am. Chem. Soc.* **2001**, *123*, 7314−7319.
(6) Guimaraes, C. R. W.; de Alencastro, R. B. *Int. J. Quantum Chem.* **2001**, *85*, 713−726.
(7) Liptak, M.; Gross, K. C.; Seybold, P. G.; Feldgus, S.; Shields, G. C. *J. Am. Chem. Soc.* **2002**, *124*, 6421−6427.
(8) Wang, T.; Brudvig, G.; Batista, V. S. *J. Chem. Theory Comput.* **2010**, *6*, 755−760.
(9) Ali, S. T.; Karamat, S.; Kóňa, J.; Fabian, W. M. *J. Phys. Chem. A* **2010**, *114*, 12470−12478.
(10) Rebollar-Zepeda, A. M.; Campos-Hernández, C.; Ramirez Silva, M. T.; Rojas-Hernández, A.; Galano, A. *J. Chem. Theory Comput.* **2011**, *7*, 2528−2538.
(11) Fifen, J. J.; Nsangou, M.; Dhaouadi, Z.; Motapon, O.; Jaidane, N. *Comput. Theor. Chem.* **2011**, *966*, 232−243.
(12) Najafi, M.; Zahedi, M.; Klein, E. *Comput. Theor. Chem.* **2011**, *978*, 16−28.
(13) Sadasivam, K.; Kumaresan, R. *Comput. Theor. Chem.* **2011**, *963*, 227−235.
(14) Altarawneh, M.; Dar, T.; Dlugogorski, B. Z. *J. Chem. Eng. Data* **2012**, *57*, 1834−1842.
(15) Marenich, A. V.; Ding, W.; Cramer, C. J.; Truhlar, D. G. *J. Phys. Chem. Lett.* **2012**, *3*, 1437−1442.
(16) Gupta, M.; da Silva, E. F.; Svendsen, H. F. *J. Phys. Chem. B* **2012**, *116*, 1865−1875.
(17) Sentil, K.; Kumaresan, R. *Comput. Theor. Chem* **2012**, *985*, 14−22.
(18) Lim, C.; Bashford, D.; Karplus, M. *J. Phys. Chem.* **1991**, *95*, 5610−5627.
(19) Tissandier, M. D.; Cowen, K. A.; Feng, W. Y.; Gundlach, E.; Cohen, M. H.; Earhart, A. D.; Coe, J. V.; Tuttle, T. R. J. *J. Phys. Chem. A* **1998**, *102*, 7787−7794.
(20) Tawa, G. J.; Topol, I. A.; Burt, S. K.; Caldwell, R. A.; Rashin, A. A. *J. Chem. Phys.* **1998**, *109*, 4852−4863.
(21) Mejias, J. A.; Lago, S. *J. Phys. Chem.* **2000**, *113*, 7306−7316.
(22) Zhan, C. G.; Dixon, D. A. *J. Phys. Chem. A* **2001**, *105*, 11534−11540.
(23) Hwang, S.; Chung, D. S. *Bull. Korean Chem. Soc.* **2005**, *26*, 589−593.
(24) Grimsrud, E. P.; Kebarle, P. *J. Am. Chem. Soc.* **1973**, *95*, 7939−7943.
(25) Fujii, A.; Enomoto, S.; Miyazaki, M.; Mikami, N. *J. Phys. Chem. A* **2005**, *109*, 138−141.
(26) Kuo, J. L.; Fujii, A.; Mikami, N. *J. Phys. Chem. A* **2007**, *111*, 9438−9445.
(27) Krishtal, A.; Senet, P.; Alsenoy, C. V. *J. Chem. Theory Comput.* **2008**, *4*, 426−434.
(28) Kaledin, M.; Wood, C. A. *J. Chem. Theory Comput.* **2010**, *6*, 2525−2535.
(29) Douberly, G. E.; Walters, R. S.; Cui, J.; Jordan, K. D.; Duncan, M. A. *J. Phys. Chem. A* **2010**, *114*, 4570−4579.
(30) Torrent-Sucarrat, M.; Anglada, J. M. *J. Chem. Theory Comput.* **2011**, *7*, 467−472.

(31) Guasco, T. L.; Johnson, M. A. *J. Phys. Chem. A* **2011**, *115*, 5847−5858.
(32) Mizuse, K.; Fujii, A. *J. Phys. Chem. Lett.* **2011**, *2*, 2130−2134.
(33) Mizuse, K.; Fujii, A. *Phys. Chem. Chem. Phys.* **2011**, *13*, 7129−7135.
(34) Mizuse, K.; Fujii, A. *J. Phys. Chem. A* **2012**, *116*, 4868−4877.
(35) Chang, H. C.; Jiang, J. C.; Lin, S. H.; Lee, Y. T.; Chang, H. C. *J. Phys. Chem. A* **1999**, *103*, 2941−2944.
(36) Chang, H. C.; Jiang, J. C.; Chang, H. C.; Wang, L. R.; Lee, Y. T. *Isr. J. Chem.* **2000**, *39*, 231−243.
(37) Landanyi, B. M.; Skaf, M. S. *Annu. Rev. Phys. Chem.* **1993**, *44*, 335−368.
(38) Tsuchida, E.; Kanada, Y.; Tsukada, M. *Chem. Phys. Lett.* **1999**, *311*, 236−240.
(39) Jellinek, J.; Beck, T. L.; Berry, R. S. *J. Chem. Phys.* **1986**, *84*, 2783−2794.
(40) Jortner, J.; Scharf, D.; Landman, U. In *Elemental and Molecular Clusters*; Benedeck, G., Martin, T. P., Pacchioni, G., Eds.; Springer: Berlin, 1988.
(41) Berry, R. S.; Beck, T. L.; Davies, H. L.; Jellinek, J. *Adv. Chem. Phys.* **1988**, *70*, 74.
(42) Berry, R. S. In *The Chemical Physics of Atomic and Molecular Clusters* Scholes, G., Ed.; North-Holland: Amsterdam, 1990.
(43) Sarkar, S.; Joarder, R. N. *J. Chem. Phys.* **1993**, *99*, 2032−2039.
(44) Wright, D.; El-Shall, M. S. *J. Chem. Phys.* **1996**, *105*, 11199.
(45) Hagemeister, F. C.; Gruenloh, C. J.; Zwier, T. S. *J. Phys. Chem. A* **1998**, *102*, 82−94.
(46) Boyd, S. D.; Boyd, R. J. *J. Chem. Theory Comput.* **2007**, *3*, 54−61.
(47) Pires, M. M.; DeTuri, V. F. *J. Chem. Theory Comput.* **2007**, *3*, 1073−1082.
(48) Ohno, K.; Shimoaka, T.; Akai, N.; Katsumoto, Y. *J. Phys. Chem. A* **2008**, *112*, 7342−7348.
(49) Liu, K.; Cruzan, J. D.; Saykally, R. J. *Science* **1976**, *271*, 929−933.
(50) Tomasi, J.; Mennucci, B.; Cammi, R. *Chem. Rev.* **2005**, *105*, 2999−3093.
(51) Frisch, M. J. et al. *Gaussian 09*, revision A.1; Gaussian Inc.: Wallingford, CT, 2009.
(52) Becke, A. *Phys. Rev.* **1998**, *A38*, 3098−3100.
(53) Lee, C.; Yang, W.; Parr, R. *Phys. Rev.* **1988**, *B37*, 785−789.
(54) Zhao, Y.; Truhlar, D. G. *Theor. Chem. Acc.* **2008**, *120*, 215−241.
(55) Chamberlin, C. A.; Cramer, C. J.; Truhlar, D. G. *J. Phys. Chem. B* **2008**, *112*, 8651−8655.
(56) Marenich, A. V.; Cramer, C. J.; Truhlar, D. G. *J. Phys. Chem. B* **2009**, *113*, 4538−4543.
(57) Clark, T.; Chandrasekhar, J.; Spitznagel, G.; Schleyer, P. *J. Comput. Chem.* **1983**, *4*, 294−301.
(58) Frisch, M.; Pople, J.; Binkley, J. *J. Chem. Phys.* **1984**, *80*, 3265−3269.
(59) Rassolov, V.; Ratner, M.; Pople, J.; Redfern, P.; Curtiss, L. *J. Comput. Chem.* **2001**, *22*, 976−984.
(60) Levenberg, K. *Q. Appl. Math.* **1944**, *2*, 164−168.
(61) Marquardt, D. *SIAM J. Appl. Math.* **1963**, *11*, 431−441.
(62) Fifen, J. J.; Nsangou, M.; Dhaouadi, Z.; Motapon, O.; Jaidane, N. *J. Chem. Phys.* **2012**, under review.
(63) Pokon, E. K.; Liptak, M. D.; Feldgus, S.; Shields, G. C. *J. Phys. Chem. A* **2001**, *105*, 10483−10487.
(64) Liptak, M. D.; Shields, G. C. *Int. J. Quantum Chem.* **2005**, *105*, 580−587.
(65) Pickard, F. C., IV; Griffith, D. R.; Ferrara, S. J.; Liptak, M. D.; Kirschner, K. N.; Shields, G. C. *Int. J. Quantum Chem.* **2006**, *106*, 3122−3128.
(66) Shields, G. C.; Kirschner, K. N. *Synth. React. Inorg., Met.-Org., Nano-Met. Chem.* **2008**, *38*, 32−39.
(67) Alongi, K. S.; Shields, G. C. *Annual Reports in Computational Chemistry*; Wheeler, R. A., Ed.; Elsevier: New York, 2010; Vol. *6*, pp 113−138.
(68) Buck, U.; Huisken, F. *Chem. Rev.* **2000**, *100*, 3863.
(69) Han, H.-L.; Camacho, C.; Witek, H. A.; Lee, Y.-P. *J. Chem. Phys.* **2011**, *134*, 11309.
(70) Afeefy, H. Y.; Liebman, J. F.; Stein, S. E. In *NIST Chemistry WebBook*, Linstrom, P. J., Mallard, W. G., Eds.; NIST Standart Reference Database Number 69, NIST: Gaithersburg, MD, 2005.
(71) Kelly, C. P.; Cramer, C. J.; Truhlar, D. G. *J. Phys. Chem. B* **2007**, *111*, 408−422.